

# Smooth joint motion planning for high precision reconfigurable robot manipulators

S. Baraldo, A. Valente, *Member, IEEE*

**Abstract**— The accuracy of reconfigurable robot manipulators is a critical aspect which prevents their diffused industrial adoption. This work presents a novel model for designing joint motion profiles, particularly suitable for the motion planning of modular robots with high accuracy requirements. The model generates smooth motion profiles, without sacrificing execution time and taking into account the different characteristics of each joint and the requirements of each production task. The proposed method has been tested across the most performing motion planning approaches found in the literature, providing up to 39% faster jerk-bounded trajectories. Moreover, the model is flexible to the generation of adapted trajectories when degrading phenomena occur over the time.

## I. MOTIVATION AND OBJECTIVE

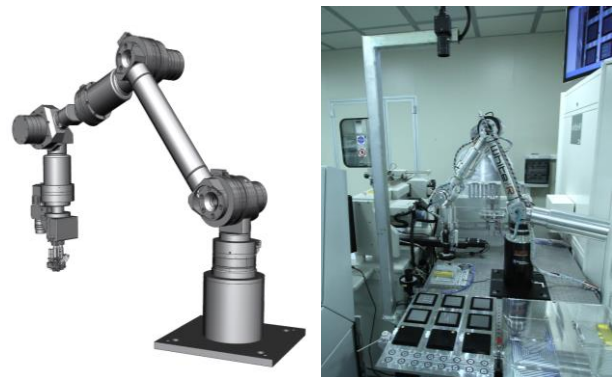
Industrial robots are demanded to target extremely challenging precision and reliability performance with agile and efficient architectures. At the same time, the reconfigurability feature for industrial robots plays an instrumental role in manufacturing contexts suffering rapid evolutions of the product geometric and technological features along with the changes in the production demand [1,2]. However, the design of reconfigurable robots for highly precise manufacturing applications still constitutes a major challenge, as the reconfigurability paradigm unlikely applies to high precision manufacturing. The foundation of such research topic covers activities related to: the design of more solid mechatronic robot modules with close to zero backlash [3]; the design of modular kinematic models which can be regenerated to adapt a robot reconfiguration [4]; the trajectory planning and path planning which can diversify the strategy to distribute the motion across the robotic chain [5]; and finally a modular control architecture that can detect and match changes of the robot morphology along with performing a persistent monitoring of its health and behaviour [3].

The present work investigates the topic of trajectory planning for reconfigurable industrial robots characterized by very high level of accuracy. The planning of trajectories and motion profiles is a critical aspect of robot control, not only because it greatly impacts the feasibility, efficiency and robustness of any motion task, but also because its goals are highly dependent on the task to be carried out. In reconfigurable robots, the aforementioned requirements are enriched with the need to take into account also the kinematic structure of the robot and the joints distribution across the robotic chain in each and every feasible configuration.

In the current work, the referred architecture of reconfigurable robot is the ReRob I that is a serial robot characterized by 5 $\mu$ m accuracy [6]. The reconfigurability of ReRob I is achieved by the modularity of both links and actuators, which can be chosen among a library of sizes and performance levels to accommodate various working tasks. Its control system architecture adopts a decentralized approach, where each sub-system (i.e. robotic joint) is an independent entity, ready to connect and interact with the entire control system (from the field up to the motion controller). By relying upon a set of KPIs, such control architecture ensures the possibility to adapt the kinematic limits of each joint and in general the trajectory of the robot, depending on the detected performance status of the robotic modules. In detail, on the subject of trajectory planning, the authors propose a time-optimal model, where smooth jerk motion profiles for the joints are efficiently synchronized. The motion profiles are optimized on the basis of the specific robot task and account for the exact allocation of the specific joint models across the robotic chain. The proposed approach is designed to support both the green field motion profile generation and the profile adaptation during the robot operating time (brown field) as a result of a detection of the robot anomalous behaviour while executing a certain task.

The rest of the paper is organized as it follows: Section II reviews the state of the art on the trajectory planning; Section III outlines the approach and model mathematical formulation; Section IV describes the results of the experimental campaign; Section V summarizes the benefits of the approach and the future steps.

Figure 1: ReRob I 3D model (left panel) and its integration in a high precision laser diode assembly workcell (right panel).



## II. LITERATURE REVIEW

The scientific subject of trajectory planning is traditionally addressed from the temporal perspective or the motion smoothness perspective. In the first case, the goal is

The authors are with the Department of Innovative Technologies (DTI), Scuola Universitaria Professionale della Svizzera Italiana, Manno, Switzerland (e-mails: [stefano.baraldo@supsi.ch](mailto:stefano.baraldo@supsi.ch), [anna.valente@supsi.ch](mailto:anna.valente@supsi.ch)).

to minimize the time necessary to execute a certain trajectory in order to match requirements of productivity [7-9]. In the case of motion smoothness of trajectories, the idea is to privilege the quality of the path and to treat the time as a constraint not to be violated [10]. There are also formulations which are a mix of the aforementioned ones [11], thus they are designed to target fast trajectories combined with optimal jerk values, in order to reduce the excitation of the resonant frequencies of the mechanical system. In this case, execution time and the norm of jerk are concurrent components of the optimized functional, so the trade-off between these two aspects has to be tuned in order to achieve the desired results.

In the field of precision manufacturing, the goal of being fast comes after the one of being stable. This motivates the authors' interest towards the smooth motion approaches while keeping the focus on the shape of the profile, and in particular on its regularity. In detail, some works rely upon the use of piecewise splines, whose coefficients are optimized with various approaches. For example, in [12] a B-spline representation of trajectories is used, and a functional that concurrently takes into account both the total execution time and the norm of jerk is minimized. The numerical minimization of the joints' jerk norm by genetic algorithms is presented in [13]. The GA approach is proposed also in [14], but in this case the chosen functional is a function of manipulability measures and thus involves the inverse kinematics. A different approach to smooth motion planning is presented in [15], where filtering on a trapezoidal motion profile is used to transform it to a more regular "exponential" motion profile.

So far, in the literature, the achievement of a smooth trajectory in the Cartesian space is translated into the joint space in a strategy of the joints movement synchronization where all the joints tune their speed on the slowest one [16] and whose higher degree of regularity is usually achieved by increasing the polynomial degree of the path or of the motion profile [17, 18, 19]. Moreover, multiple-axis movements are often managed in the operations workspace [20], although the definition of trajectories in joint space is in some cases a viable simplification that allows to implement smoother joint trajectories. A further limit for the robot motion capability is represented by the impossibility to adapt the motion planning strategies on the fly if a robot anomaly is detected at servo drives or CNC levels. As a result of that, the degrading phenomena of robots cannot be minimized or temporarily handled with a regenerative motion strategy that is optimized over the time.

### III. TRAJECTORY PLANNING

The model detailed in the current section is based on the optimization of execution time and smoothness by generating trajectories in the joint space from a *sine-jerk* model, under the constraint of given maximum values for acceleration, velocity and jerk. Compared to the current state of the art, and in particular with respect to [16], which adopts a similar approach, the proposed work presents a number of novel features:

- All available Degrees of Freedom (*DoF* in the following) are exploited when executing a manufacturing task in order to rely upon a more

flexible infrastructure associated to all the viable configurations of the same robot; such approach is traditionally avoided in the literature as high precision tasks are performed, whenever possible, by manipulators with the least possible number of *DoF*.

- In [16], joints are coordinated by synchronizing each phase of the trajectory (acceleration, constant velocity and deceleration) across all the joints, and by imposing the duration of each phase to the longest time evaluated on joints considered singularly. The proposed approach, on the contrary, constraints only the total movement duration to be equal for all the joints, and optimizes time basing on the remaining trajectory parameters.
- Velocity, acceleration and jerk bounds are satisfied rigorously, while the approach exposed in [16] does not guarantee that velocity remains within the given limits.
- The motion planning embeds also the information about the joints' positions on the kinematic chain, thus preferring to distribute the motion towards the robot basis rather than to the nose.
- The motion planning is adaptive towards the joint degrading process and enables the implementation of logics that prevent the occurrence of critical failures and parts which are out of control. Specifically, based on the control architecture, each joint communicates continuously to the motion controller its local KPIs (e.g. position error, velocity and acceleration, absorbed electrical power or drive temperature), thus enabling a persistent monitoring of the robot health based on a continuous analysis of the trends of their rate of change while carrying out both repetitive and disparate tasks over time. In fact, in the case any anomaly would occur, the controller generates a recovery strategy by adapting the kinematic limits of each joint, depending on the detected performance status (green field or brown field).
- The motion planning also considers the reconfiguration of the robotic structure where a certain joint can be replaced by different ones in the same location of the robotic chain and, consequently, the motion strategy must be regenerated.

#### A. Model assumptions

In the current work, the trajectory planning module that will be introduced refers to the following assumptions:

1. The robot manipulator of interest performs mainly pick-and-place tasks in which *rapid* movements are required to be as smooth as possible, to provide a high degree of stability of the gripped component.
2. Rapid movements are performed between pre-pick and pre-place positions, which do not require specific paths (e.g. linear) in the Cartesian workspace. Moreover, no obstacles are present within the workcell. This implies that rapid point-to-point movements can be performed by trajectories designed in the joints space.

3. The focus will be given to the example of a specific configuration of ReRob I, a 6-DoF anthropomorphic manipulator with spherical wrist, although the proposed motion profile design method is of general purpose, and it can be adapted to any serial or parallel manipulator with arbitrary DoFs. This degree of generality is especially useful for modular reconfigurable robots, where motion planning should be flexible enough to adapt to various kinematic chains.

Assumptions 2 (on the obstacle absence if the model is enriched with boundary constraints) and 3 have been formulated for the sake of brevity. However, the model can be easily scaled up to more comprehensive applications where such constraints are relaxed.

### B. Model description

As anticipated in Section I, the reconfigurability of ReRob I is achieved by the modularity of both links and actuators, which can be chosen among a library of sizes and performance levels to accommodate various working tasks. Each joint  $i = 1, \dots, 6$ , where the index  $i$  represents the serial position in the kinematic chain, is characterized by specific a joint type  $k_i$ . In particular, a typical anthropomorphic, spherical-wrist configuration of ReRob I is assembled by using 2 different types of joints: a higher torque model for the first 3 axes and a smaller, lower torque model for the 3 wrist axes, yielding  $k_1, k_2, k_3 = 1$  and  $k_4, k_5, k_6 = 2$ . Each joint has different velocity, acceleration and jerk ranges, depending on the type of joint and on the position in the kinematic chain.

Also the specific type of production task and the starting and ending positions may influence the kinematic parameters for each joint: for example, movements to be performed with the gripper empty may be realized at higher speeds and accelerations with respect to movements performed carrying a component; moreover, long-reach trajectories, which are more stressful for the actuators, may require slower movements to keep oscillations within the required specifications. For this reason, we introduce also a task index  $m = 1, \dots, n_t$ , which allows to differentiate control parameters between different segments of the work process. As mentioned before, this index depends on starting and ending positions  $\underline{p}_s, \underline{p}_e$  and task type  $h$  (e.g. pick, place, change tool), but for brevity the full dependence  $m = m(\underline{p}_s, \underline{p}_e, h)$  will be omitted in the following.

While executing a certain manipulation task, the robot trajectory can be modelled as a point-to-point move characterized by its starting and ending positions in the workspace expressed by 6 coordinates in the Cartesian space ( $x, y, z$  and 3 angles  $a, b, c$  describing completely the end effector state as a rigid body). A spherical wrist 6-axis robot can reach any position within its workspace by at most 8 different postures, i.e. all the combinations of these 3 alternatives [21]:

- shoulder to the right/to the left,
- elbow to the right/to the left,
- flipped/un-flipped wrist.

The 8 posture versions of the starting and ending pose are computed, yielding a total of 64 posture-to-posture solutions. These combinations can be realized by very different sets of joint angles. Generally, not all of these postures can be reached by the robot, due to joint range limitations. We consider 2 reasons for limiting the joints ranges:

- mechanical limitations (e.g. auto-collision, cable wrapping),
- singularity avoidance (e.g. shoulder, elbow and wrist singularities for a spherical wrist, anthropomorphic manipulator [21]).

Among the possible posture-to-posture combinations, the ones that are unfeasible for any of the above reasons are filtered out, thus reducing the total number of options.

### C. Sine-Jerk Motion Profile mathematical formulation

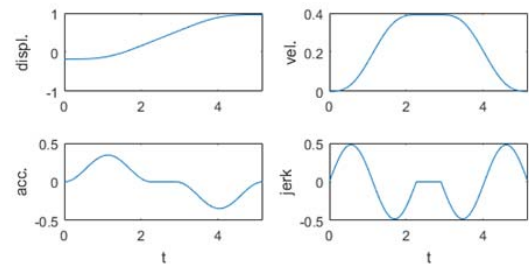
For every feasible alternative pose of the robot, translated into a starting and ending position of each joint, the following step is to generate the motion profiles for the joints. The algorithm we propose generates trajectories in the joint space, with motion profiles that are monotonic for each single joint. The pose which will be selected among the alternatives will be the one ensuring the execution time and smoothness.

To generate joint motion profiles, we choose an expression of jerk as a function of time suggested in [22]. The proposed profile for a single motor, exemplified in Figure 2, is

$$j(t) = \begin{cases} J \sin\left(\frac{2\pi}{T_A} t\right) & \text{for } t \in [0, T_A) \\ 0 & \text{for } t \in [T_A, T_A + T_V) \\ -J \sin\left(\frac{2\pi}{T_A} t\right) & \text{for } t \in [T_A + T_V, 2T_A + T_V], \end{cases} \quad (1)$$

where  $J$  is the jerk peak value,  $T_A$  is the acceleration time and  $T_V$  is the constant velocity time.

Figure 2: jerk, acceleration, velocity and displacement derived from the sinusoidal jerk model.



Notice that  $2\pi/T_A$  represents the sine-wave angular frequency. This profile exhibits very high regularity, nonetheless it allows to parametrize the displacement, velocity and acceleration profiles by few, easily interpretable parameters, and to optimize efficiently over them.

### D. Joint Optimization of Motion Profiles

Let us define  $D$  as the total required (angular) displacement for a single joint. By integration and some algebraic manipulation, we obtain the following expressions for the dynamic control parameters (see Appendix A for details):

$$\text{Peak acceleration} \quad A = \frac{JT_A}{\pi} \quad (2)$$

$$\text{Peak velocity} \quad V = \frac{JT_A^2}{2\pi} \quad (3)$$

$$\text{Constant velocity time} \quad T_V = D \frac{2\pi}{JT_A^2} - T_A. \quad (4)$$

To perform the smoothest possible trajectory and to avoid inducing unnecessary stresses or vibrations to the robot arm, we synchronize the motion profiles of all joints to complete the move at the same time, while limiting jerk, acceleration and velocity to remain under fixed values. This corresponds to set up a nonlinear constrained optimization problem, which takes into account all the 6 joints' motion profiles at once and, concurrently, leverages the motion capabilities on the relative joint position in the kinematic chain (indexed as  $i = 1, \dots, 6$  in the following), as well as the specific task requirements (indexed as  $j = 1, \dots, n_t$ ). A re-parametrization of the quantities of interest as functions of the total move time  $T = 2T_A + T_V$  and of the 6 acceleration times  $T_A = (T_{A1}, \dots, T_{A6})$  (see Appendix B) allows to set up the following optimization problem, structured with the objective function (5) that minimizes the execution time under the following constraints: positive execution time (6) and acceleration times (7); accomplishment of the jerk limits (8), acceleration limits (9) and velocity limits (10); total execution time at least double compared to the acceleration time (11):

for any fixed task  $m \in \{1, \dots, n_t\}$ ,

$$\min_{T_A, T_m} T_m \quad (5)$$

subject to

$$T_m \geq 0, \quad (6)$$

$$T_{Ami} \geq 0, \quad (7)$$

$$-J_{mi}^{MAX} \leq J(T_m, T_{Ami}) = \frac{2\pi D}{T_{Ami}^2(T_m - T_{Ami})} \leq J_{mi}^{MAX}, \quad (8)$$

$$-A_{mi}^{MAX} \leq A(T_m, T_{Ami}) = \frac{2D}{T_{Ami}(T_m - T_{Ami})} \leq A_{mi}^{MAX}, \quad (9)$$

$$-V_{mi}^{MAX} \leq V(T_m, T_{Ami}) = \frac{D}{T_m - T_{Ami}} \leq V_{mi}^{MAX}, \quad (10)$$

$$0 \leq T_V(T_m, T_{Ami}) = T_m - 2T_{Ami}, \quad (11)$$

for all joints  $i = 1, \dots, 6$ .

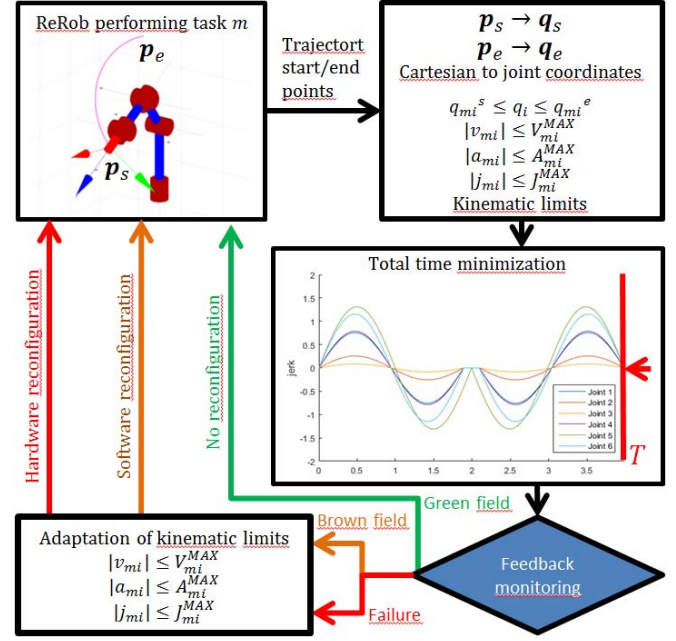
Notice that the total execution time  $T_m$  is common to all the joints, while the acceleration times  $T_{Ami}$  are different. The beginning and ending of the movement are synchronized across the 6 joints' motion profiles, but since the synchronization is a constraint of the optimization (all the joints complete the movement at the same time  $T_m$ ), the control parameters are automatically adapted to the best acceptable performance, instead of simply rescaling all the profiles with respect to the slowest one. The simultaneous motion of all joints provides a higher degree of regularity to the global trajectory, since no acceleration spikes of single joints are present during the movement.

The functional to optimize is linear, and it can be proved that all the constraints are convex, so any local minimizer is also a global one. This optimization problem can be solved quickly, for example, using an active-set algorithm [23].

The formulation described by (5)-(11) is such that it is easy to implement limitations to kinematic quantities,

specific for each joint position and type. This allows to apply highly customized joint management approaches, like for example the one suggested in [1] to perform operations in a "degraded" mode by redistributing the workload to motors that perform better. A diagram of the adaptation loop is presented in Figure 3, while a simulated example of this operation mode is presented in Section IV.

Figure 3: parameter adaptation scheme.



#### IV. SIMULATION

The proposed motion planning method has been tested by simulations performed with Matlab<sup>®</sup>. The kinematics of a 6-DoF, spherical wrist anthropomorphic robot has been reproduced and represented using the toolbox proposed in [24].

The method presented in this work has been compared with a number of benchmark methods, namely [10,16,25,26,27]. These papers consider two benchmark point-to-point trajectories. In detail, TABLE I presents the data sets considered in [10,16,25,26]; TABLE II outlines the data sets considered in [16,27]. The results of the comparison are proposed in TABLE III.

The method proposed in this work yields much lower execution times with respect to all the considered works, including [16], which adopts the same kind of jerk profiles but uses a different synchronization method. This result is achieved by pushing each joint to its best possible performance, but without violating any given constraint. In fact, as an example for the data set belonging to Table I, if the upper bound of the jerk value is  $60^\circ/\text{s}^3$  (i.e. a value compatible with the top ReRob I joint performance), the resulting execution time is 39% lower than the results by [16], thanks to the full exploitation of the allowed jerk range; if this jerk upper bound is set as equal to the one obtained in [16], the same execution time is achieved: this highlights the fact that [16] represents a less general, conservative method with respect to the one proposed in this work.

TABLE I. TEST TRAJECTORY AND KINEMATIC CONSTRAINTS, DATASET 1

Joint		1	2	3	4	5	6
Position	Initial [rad]	0	$-\pi/6$	0	$-\pi/3$	0	0
	Final [rad]	$2\pi/3$	$\pi/6$	$\pi/4$	$\pi/3$	$-\pi/4$	$\pi/6$
Constraint	Velocity [rad/s]	8	10	10	5	5	5
	Acceleration [rad/s <sup>2</sup> ]	10	12	12	8	8	8
	Jerk [rad/s <sup>3</sup> ]	30	40	40	20	20	20

TABLE II. TEST TRAJECTORY AND KINEMATIC CONSTRAINTS, DATASET 2

Joint		1	2	3	4	5	6
Position	Initial [°]	-10	20	15	150	30	120
	Final [°]	55	35	30	10	70	25
Constraint	Velocity [°/s]	100	95	100	150	130	110
	Acceleration [°/s <sup>2</sup> ]	60	60	75	70	90	80
	Jerk [°/s <sup>3</sup> ]	60	66	85	70	75	70

TABLE III. SIMULATION RESULTS COMPARISON

Data	Work	Performance measure	
		Ex. Time	Max jerk
1	Gasparetto and Zanotto	9.1s	46.85°/s <sup>3</sup>
	Piazzini and Visioli	9.1s	49.35°/s <sup>3</sup>
	Simon and Isik	9.1s	80.8°/s <sup>3</sup>
	Perumaal and Natarajan	7.5398s	16.4178°/s <sup>3</sup>
	Baraldo and Valente, full constraints	4.6498s	60°/s <sup>3</sup> (Joint 1)
	Baraldo and Valente, jerks limited to 60°/s <sup>2</sup>	7.3885s	16.0000°/s <sup>3</sup> (Joint 1)
2	Chettibi et al.	2.675s	30rad/s <sup>3</sup>
	Perumaal and Natarajan	2.5133s	6.63rad/s <sup>3</sup>
	Baraldo and Valente, full constraints	1.7395s	20rad/s <sup>3</sup> (Joint 4)
	Baraldo and Valente, jerks limited to 6.60rad/s <sup>2</sup>	2.2236s	6.60rad/s <sup>3</sup> (Joint 4)

Since kinematic bounds are explicit model parameters and they are always satisfied by the calculated trajectory, the proposed model is particularly suitable for an easy implementation of any variation of kinematic performance parameters, targeting specific joints. Such feature comes extremely instrumental in robots which are reconfigurable as it enables the identification of degrading patterns of joints and the consequent temporary adaptation (scale down) of motion logics till the joint is not substituted. In detail, since the execution time is optimized by taking into account all the joints simultaneously, the overall performance of the joints is downscaled enough to accommodate the synchronization of all joints, but avoiding unnecessary proportional, global overrides which is typical of traditional robotic chains. An example of this feature in action is presented in TABLE IV, where the normal sine-jerk trajectory for the Dataset 2 is compared with various degraded versions: one obtained under limited jerk (e.g. because of excessive vibrations detected), one obtained with limited acceleration and one

given by a lower velocity constraint (e.g. for anomalies in the motor performance).

TABLE IV. PERFORMANCES WITH DEGRADED JOINTS (DATASET 2)

Condition	Performance measure	
	Ex. time	Max jerk
Nominal	1.7395s	20rad/s <sup>3</sup> (Joint 4)
Jerk of J4 degraded from 20 to 5rad/s <sup>3</sup>	2.7613s	5rad/s <sup>3</sup> (Joint 4)
Acceleration of J3 degraded from 12 to 1rad/s <sup>2</sup>	2.5066s	6.6843rad/s <sup>3</sup> (Joint 4)
Velocity of joint 1 degraded from 8 to 0.5rad/s	4.5124s	30rad/s <sup>3</sup> (Joint 1)

## V. CONCLUSION

The proposed method allows to set up smooth motion profiles for each single joint of ReRob I, a reconfigurable robot manipulator. The control parameters are implemented in a simple and direct way, allowing to customize the robot's kinematic behaviour during each trajectory while taking into account specific requirements associated to the type of joint and the production task to be accomplished. For the benchmark dataset, this approach yields execution times more than 39% shorter than the best state of the art method, while maintaining the motion profiles as smooth as desired. Future works will include the implementation of obstacle avoidance; moreover, the formulation could be extended to more general motion profiles characterized by a continuous path of the robot, thus going through intermediate points that present arbitrary values of velocity, acceleration and jerk.

## APPENDIX

### A. Analytical forms of kinematic quantities

Given the expression of the jerk as a scaled sine with a given frequency, we describe in the following how to obtain the maximum acceleration and velocity, as well as the displacement during the acceleration phase. For the sake of simplicity, joint indices are omitted in the following formulas.

The peak acceleration is obtained when the jerk completes its positive phase, i.e. at  $t = T_A/2$ . By integration, the general expression of acceleration within  $t \leq T_A$  is

$$\begin{aligned}
 a(t) &= \int_0^t J \sin\left(\frac{2\pi}{T_A}s\right) ds = \frac{JT_A}{2\pi} \left[ -\cos\left(\frac{2\pi}{T_A}s\right) \right]_0^t \\
 &= \frac{JT_A}{2\pi} \left[ -\cos\left(\frac{2\pi}{T_A}s\right) \right]_0^t \\
 &= \frac{JT_A}{2\pi} \left[ 1 - \cos\left(\frac{2\pi}{T_A}t\right) \right], \quad t \leq T_A,
 \end{aligned} \tag{12}$$

which becomes, evaluated at  $t = T_A/2$ ,

$$A = a\left(\frac{T_A}{2}\right) = \frac{JT_A}{2\pi} [1 - \cos(\pi)] = \frac{JT_A}{2\pi}. \tag{13}$$

The peak velocity (the one that is maintained during the middle segment of the motion profile) is reached at the end of the positive acceleration phase. By integration, the general expression of velocity within  $t \leq T_A$  is

$$v(t) = \frac{JT_A}{2\pi} \int_0^t \left[ 1 - \cos\left(\frac{2\pi}{T_A}s\right) \right] ds$$



$$\begin{aligned}
&= \frac{JT_A}{2\pi} \left[ s - \frac{T_A}{2\pi} \sin\left(\frac{2\pi}{T_A} s\right) \right]_0^t \\
&= \frac{JT_A}{2\pi} \left[ t - \frac{T_A}{2\pi} \sin\left(\frac{2\pi}{T_A} t\right) \right], \quad t \leq T_A,
\end{aligned} \quad (14)$$

which becomes, evaluated at  $t = T_A$ ,

$$V = v(T_A) = \frac{JT_A}{2\pi} \left[ T_A - \frac{T_A}{2\pi} \sin(2\pi) \right] = \frac{JT_A^2}{2\pi}. \quad (15)$$

The displacement in the acceleration phase ( $t \leq T_A$ ) is

$$\begin{aligned}
d(t) &= \frac{JT_A}{2\pi} \int_0^t \left[ s - \frac{T_A}{2\pi} \sin\left(\frac{2\pi}{T_A} s\right) \right] ds \\
&= \frac{JT_A}{2\pi} \left[ \frac{s^2}{2} + \frac{T_A^2}{4\pi^2} \cos\left(\frac{2\pi}{T_A} s\right) \right]_0^t \\
&= \frac{JT_A}{2\pi} \left[ \frac{t^2}{2} + \frac{T_A^2}{4\pi^2} \cos\left(\frac{2\pi}{T_A} t\right) - \frac{T_A^2}{4\pi^2} \right], \quad t \leq T_A,
\end{aligned} \quad (16)$$

which becomes, evaluated at  $t = T_A$ ,

$$D_A = d(T_A) = \frac{JT_A}{2\pi} \left[ \frac{T_A^2}{2} + \frac{T_A^2 \cos(2\pi)}{4\pi^2} - \frac{T_A^2}{4\pi^2} \right] = \frac{JT_A^3}{4\pi}. \quad (17)$$

Being in the constant velocity phase  $T_V = \frac{D_V}{V}$ , by substitution we obtain

$$T_V = \frac{D - 2D_A}{V} = \frac{D - \frac{JT_A^3}{4\pi}}{\frac{JT_A^2}{2\pi}} = \frac{2\pi D}{JT_A^2} - T_A. \quad (18)$$

### B. Total Time and Sine Period parametrization

The total move is composed by the constant velocity phase and the acceleration and deceleration phases, which are symmetrical and thus have the same duration. This yields

$$T_V = T - 2T_A. \quad (19)$$

By comparing (18) and (19), we can express the jerk as a function of  $T$  and  $T_A$

$$J = \frac{2\pi D}{T_A^2(T - T_A)}. \quad (20)$$

### ACKNOWLEDGMENT

The research funded in this paper has been partially supported by EU FoF 2012 Project whiteR — white room based on Reconfigurable robotic Island for optoelectronics. Contract 609228.

### REFERENCES

- [1] A. Valente, "Reconfigurable Industrial Robots: A Stochastic Programming approach for designing and assembling robotic arms", *Robotics and Computer-Integrated Manufacturing*, vol. 41, pp. 115–126, 2016.
- [2] M. Yim, W. Shen, B. Salemi, D. Rus, M. Moll, H. Lipson, E. Klavins and G. Chirikjian, "Modular self-reconfigurable robot systems", *IEEE Robotics and Automation Magazine*, vol. 14, no. 1, pp. 43–52, 2007.
- [3] A. Valente, "Design and optimization of compact and lightweight modular joints for High Accuracy Reconfigurable Industrial Robots", in *Industrial Technologies 2016*, Amsterdam, 22–24 June, 2016.
- [4] Z. M. Bi and W. J. Zhang, "Concurrent Optimal Design of Modular Robotic Configuration", *Journal of Robotic Systems*, vol. 18, no. 2, pp. 77–87, 2000.
- [5] O. Avram and A. Valente, "Trajectory Planning for Reconfigurable Industrial Robots Designed to Operate in a High Precision Manufacturing Industry", 49th CIRP Conference on Manufacturing Systems, Stuttgart, 25–27 May 2016.

- [6] A. Valente, "Reconfigurable Industrial Robots – an integrated approach to design the joint and link modules and configure the robot manipulator", *3rd IEEE/IFToMM International Conference on Reconfigurable Mechanisms and Robots*, Beijing, China, 20–22 July 2015.
- [7] J. Kim, S. R. Kim, S. J. Kim and D. H. Kim, "A practical approach for minimum-time trajectory planning for industrial robots", *Industrial Robot: An International Journal*, vol. 37, pp. 51–61, 2010.
- [8] D. Constantinescu and E. A. Croft, "Smooth and time-optimal trajectory planning for industrial manipulators along specified paths", *Journal of Robotic Systems*, vol. 17 pp. 233–249, 2000.
- [9] G. Antonelli, S. Chiaverini, P. Gerio, M. Palladino and G. Renga, "SmartMove4: an industrial implementation of trajectory planning for robots", *Industrial Robot: An International Journal*, vol. 34, pp. 217–224, 2007.
- [10] A. Piazzoli, A. Visioli, "Global Minimum-Jerk Trajectory Planning for Robot Manipulators", *IEEE Transactions on Industrial Electronics*, vol. 47, no. 1, pp. 140–149, 2000.
- [11] A. Gasparetto, A. Lanzutti, R. Vidoni and V. Zanutto, "Experimental validation and comparative analysis of optimal time-jerk algorithms for trajectory planning", *Robotics and Computer-Integrated Manufacturing*, vol. 28, pp. 164–181, 2012.
- [12] A. Gasparetto and V. Zanutto, "A new method for smooth trajectory planning of robot manipulators", *Mechanism and Machine Theory*, vol. 42, pp. 455–471, 2007.
- [13] P. Huang, K. Chen, J. Yuan and Y. Xu, "Motion Trajectory Planning of Space Manipulator for Joint Jerk Minimization", *Proceedings of the 2007 IEEE International Conference on Mechatronics and Automation*, Harbin, China, August 5–9, 2007.
- [14] X. F. Zha, "Optimal pose trajectory planning for robot manipulators", *Mechanism and Machine Theory*, vol. 37, pp. 1063–1086, 2002.
- [15] L. Biagiotti, C. Melchiorri, L. Moriello, "Optimal Trajectories for Vibration Reduction Based on Exponential Filters", *IEEE Trans. Contr. Sys. Techn.* vol. 24, num. 2, pp. 609–622, 2016.
- [16] S. Perumaal and N. Jawahar, "Synchronized trigonometric S-curve trajectory for jerk-bounded time-optimal pick and place operation", *Int J of Robotics & Automation*, vol. 27, no. 4 pp. 385–395, 2012.
- [17] S. Macfarlane and E. A. Croft, "Jerk-bounded manipulator trajectory planning: design for real-time applications", *IEEE Transactions on Robotics and Automation*, vol. 19, pp. 42–52, 2003.
- [18] N. D. Nguyen, T. Ng and I. Chen, "On Algorithms for Planning S-curve Motion Profiles", *International Journal of Advanced Robotic Systems*, vol. 5, pp. 99–106, 2008.
- [19] C. D. Porawagama, "Reduced jerk joint space trajectory planning method using 5-3-5 spline for robot manipulators", *7th International Conference on Information and Automation for Sustainability*, Colombo, Sri Lanka, December 22–24, 2014.
- [20] C. Rossi and S. Savino, "Robot trajectory planning by assigning positions and tangential velocities", *Robotics and Computer-Integrated Manufacturing*, vol. 29, pp. 130–156, 2013.
- [21] B. Siciliano, L. Sciacivico, L. Villani and G. Oriolo, *Robotics. Modelling, Planning and Control*, Chapter 3, Springer-Verlag London, 2009.
- [22] H. Li, M. D. Le, Z. M. Gong and W. Lin, "Motion Profile Design to Reduce Residual Vibration of High-Speed Positioning Stages", *IEEE/ASME Transactions on Mechatronics*, vol. 14, no. 2, pp. 264–269, Apr. 2009.
- [23] J. Nocedal and S. J. Wright, *Numerical Optimization, Chapter 16*, Springer-Verlag, New York, 1999.
- [24] P.I. Corke, *Robotics, Vision & Control*, Springer 2011.
- [25] A. Gasparetto and V. Zanutto, "A technique for time-jerk optimal planning of robot trajectories", *Robotics and Computer-Integrated Manufacturing*, vol. 24, pp. 415–426, 2008.
- [26] D. Simon and C. Isik, "A trigonometric trajectory generator for robotic arms", *International Journal of Control*, vol. 57, no. 3, pp. 505–517, 1993.
- [27] T. Chettibi, H.E. Lehtihet, M. Haddad and S. Hanchi, "Minimum cost trajectory planning for industrial robots", *European Journal of Mechanics-A/Solids*, vol. 23, pp. 703–715, 2004.